Title page

Pulmonary artery wave propagation and reservoir function in conscious man: impact of pulmonary vascular disease, respiration and dynamic stress tests

Junjing Su[1,2], Charlotte Manisty[3], Ulf Simonsen[1], Luke S. Howard[2], Kim H. Parker[4], Alun D. Hughes[2,3]

[1]Department of Biomedicine, Aarhus University

[2]National Heart and Lung Institute, Imperial College London

[3]Institute of Cardiovascular Science, University College London

[4]Department of Bioengineering, Imperial College London

Running title: WIA and reservoir-excess pressure analysis in the pulmonary artery

Key words: pulmonary circulation, hemodynamics, pulse wave analysis

Table of contents category: cardiovascular

Correspondence:

Junjing Su, MD

Department of Biomedicine – Pharmacology

Aarhus University

Wilhelm Meyers Allé 4

8000 Aarhus C

Denmark

Email: junjing.su@biomed.au.dk

Tlf. + 45 8716 7692

Key points

- Wave travel plays an important role in cardiovascular physiology. However, many aspects of pulmonary arterial wave behaviour remain unclear
- Wave intensity and reservoir-excess pressure analyses were applied in the pulmonary artery in subjects with and without pulmonary hypertension during spontaneous respiration and dynamic stress tests.
- Arterial wave energy decreased during expiration and Valsalva manoeuvre due to decreased ventricular preload. Wave energy also decreased during handgrip exercise due to increased heart rate.
- In pulmonary hypertension patients, the asymptotic pressure at which the microvascular flow ceases, the reservoir pressure related to arterial compliance and the excess pressure caused by waves increased. The reservoir and excess pressures decreased during Valsalva manoeuvre but remained unchanged during handgrip exercise.
- This study provides insights into the influence of pulmonary vascular disease, spontaneous respiration and dynamic stress tests on pulmonary artery wave propagation and reservoir function.

Abstract

Detailed hemodynamic analysis may provide novel insights into the pulmonary circulation. Therefore, wave intensity and reservoir-excess pressure analyses were applied in the pulmonary artery to characterise changes in wave propagation and reservoir function during spontaneous respiration and dynamic stress tests. Right heart catheterisation was performed using a pressure and Doppler flow sensor tipped guidewire to obtain simultaneous pressure and flow velocity measurements in the pulmonary artery in control subjects and patients with pulmonary arterial hypertension (PAH) at rest. In controls, recordings were also obtained during Valsalva manoeuvre and handgrip exercise. The asymptotic pressure at which the flow through the microcirculation ceases, the reservoir pressure related to arterial compliance and the excess pressure caused by arterial waves increased in PAH patients compared to controls. The systolic and diastolic rate constants also increased, while the diastolic time constant decreased. The forward compression wave energy decreased by ~6 % in controls and ~5 % in PAH patients during expiration compared to inspiration, while the wave speed remained unchanged throughout the respiratory cycle. Wave energy decreased during Valsalva manoeuvre (by ~50 %) and handgrip exercise (by ~27 %) with unaffected wave speed. Moreover, the reservoir and excess pressures decreased during Valsalva manoeuvre but remained unaltered during handgrip exercise. In conclusion, reservoir-excess pressure analysis applied to the pulmonary artery revealed distinctive differences between controls and PAH patients. Variations in the ventricular preload and afterload influence pulmonary arterial wave propagation as demonstrated by changes in wave energy during spontaneous respiration and dynamic stress tests.

Abbreviations

BCW, backward compression wave; BDW: backward decompression wave; C, compliance; c, wave speed; CCD; duration of cardiac cycle; ERPI, excess reservoir pressure index; FCW, forward compression wave; FDW, forward decompression wave; k_d, diastolic rate constant; k_s, systolic rate constant; P, pressure; PAH: pulmonary arterial hypertension; PAPm: mean pulmonary arterial pressure; pPAP, pulmonary arterial pulse pressure; P_r, reservoir pressure; PVR, pulmonary vascular resistance; P_x, excess pressure; P_∞: asymptotic pressure; TPR: total pulmonary resistance, R, resistance; RC, product of resistance and compliance; ρ, blood density; RV, right ventricle; τ, diastolic time constant; U, velocity; WIA, wave intensity analysis; WRI: wave reflection index; Z_c, characteristic impedance.

Introduction

Wave propagation and Windkessel models are widely used to describe the arterial system. In 1-dimensional wave propagation models, the artery is envisaged as an elastic tube, where travelling waves occur. The speed at which the wave travels through the arterial tree is a surrogate marker for arterial stiffness. Wave intensity analysis (WIA) (Parker, 2009;Su *et al.*, 2016) is an investigative tool that uses simultaneous changes in the arterial pressure and flow velocity to determine the intensity, origin, type and timing of the arterial waves. Four types of arterial waves are described: forward waves are generated by upstream events, e.g. related to the ventricle (and reflections of backward waves) and can be a forward compression wave (FCW) that increases the pressure and flow or a forward decompression wave (FDW) that decreases the pressure and flow. Similarly, backward waves are generated by downstream properties and can be a backward compression wave (BCW) that increases the pressure while decreasing the flow or a backward decompression wave (BDW) that decreases the pressure while increasing the flow.

In the Windkessel model, large elastic arteries are modelled as a single compliant compartment. When the ventricle ejects blood into this compartment, arterial inflow temporarily exceeds outflow leading to increased compartmental volume, the reservoir volume, and the reservoir pressure is the pressure that has to build up to store the reservoir volume. The Windkessel model is a simple model that is easy to understand, but cannot take account of wave phenomena. More recently, a model which incorporates features of the Windkessel model with the wave propagation model has been developed (Wang *et al.*, 2003) and after modification has been termed the reservoir-excess pressure model (Parker, 2013).

In recent years, there is an increasing interest in the role of travelling waves in arterial physiology and pathophysiology. For instance, WIA applied in animal models has provided novel insights into the arterial properties of the adult and fetal pulmonary circulation (Hollander *et al.*, 2004;Smolich *et*

al., 2008). Recently, several studies have explored the usefulness of WIA in pulmonary hypertension (defined as a mean pulmonary arterial pressure, PAPm ≥ 25 mmHg) (Lau *et al.*, 2014;Quail *et al.*, 2015) (Su *et al*. 2017, submitted). However, there are still many aspects of wave propagation in the pulmonary artery that remain unclear. The objective of this study was to employ WIA and reservoir-excess pressure analysis in the pulmonary artery in subjects with and without pulmonary arterial hypertension (PAH) to characterise wave propagation and reservoir function during spontaneous respiration and dynamic stress tests in the forms of Valsalva manoeuvre and handgrip exercise.

Methods

Ethical approval

Control subjects were selected among patients that were referred for coronary angiography or electrophysiology procedures for supraventricular tachycardias. Patients without significant cardiovascular or lung diseases that had unobstructed coronary arteries on the angiogram and normal biventricular dimensions and function without significant valvular pathology as assessed by transthoracic echocardiography were included as controls. PAH patients were recruited from the National Pulmonary Hypertension Service. The study conformed to the Declaration of Helsinki and was approved by the London-Fulham Research Ethics Committee (reference 13/LO/1305) and all of the subjects gave written informed consent.

Study protocol

All patients were in sinus rhythm at the time of investigation. Right heart catheterisation was performed by advancing a 6 Fr multipurpose catheter or a 6 Fr balloon flotation catheter into either

the left or right pulmonary artery via the right femoral or brachial vein. A combined dual-tipped pressure and Doppler flow sensor wire (Combowire, Philips Volcano, California, USA) was then advanced approximately 1 cm beyond the end of the catheter (Su *et al*. 2017, submitted). Careful manipulation of the catheter and wire ensured that the Doppler flow velocity signals were optimized *in situ*. Once stable signals were observed, pressure and velocity data were acquired simultaneously (Combomap, Philips Volcano) at a sampling rate of 200 Hz for 30 – 60 seconds together with ECG monitoring in free breathing state. Subsequently, the control subjects were asked to perform a modified Valsalva Manoeuvre by exhaling against a custom-designed pressure device to maintain a target pressure of 30 mmHg for 10 – 15 seconds. After returning to resting condition, the recordings were made for 20 seconds during submaximal (50 %) isometric handgrip exercise. Cardiac output at rest was determined by direct Fick method. If direct measurement was not possible, the indirect Fick method was used.

Wave intensity analysis

WIA was performed using custom-written Matlab software (MathWorks, Massachusetts, USA). Pressure and velocity signals were ensemble-averaged by an automated process using the R-wave on the ECG as a fiducial marker. The signals were smoothed and the 1st derivative of the data was calculated using a Savitzky-Golay differentiating filter (2nd order polynomial fit, window size 11). Hardware-related delay between pressure and velocity signals was corrected by shifting the velocity data until the beginning of the upslope of the velocity and pressure waveforms were aligned (Su *et al*., 2017, submitted).

The net wave intensity is the product of the measured change in pressure and velocity and describes the rate of wave energy flux per cross sectional area of the artery. It is positive for forward travelling waves and negative for backward travelling waves. The local wave speed (c) was calculated using the sum of squares method (equation 1) (Davies *et al.*, 2006).

(1) $$c = \frac{1}{\rho} \cdot \sqrt{\frac{\sum dP^2}{\sum dU^2}}$$

where ρ is the blood density, assumed to be 1040 kg/m^3 and the sum is taken over one cardiac period.

The original dimension of wave intensity depends on the sampling time of data acquisition and therefore, "time-normalized" wave intensity calculated using the derivatives of pressure and velocity was derived (Parker, 2009). However, the resulting dimension for the time-normalized value ($Wm^{-2}s^{-2}$) does not have a straightforward physiological meaning. To circumvent this problem, here, wave intensity (WI) was normalized to the number of samples squared in the cardiac cycle. Given that analyses were performed on complete cardiac cycles, this is a more "natural" normalization than time normalization; however it is simple to convert between time- and cycle-normalized units, if required, using the duration of the cardiac cycle. Separation of waves into their forward (WI_+) and backward (WI_-) components was performed (equation 2).

(2) $$WI_{\pm} = \pm\left(\frac{dP}{dt} \pm \rho c \cdot \frac{dU}{dt}\right)^2 \cdot CCD^2 \Big/ (4\rho c)$$

where CCD is the duration of the cardiac cycle.

To assess the respiratory variation, cardiac beats were identified as inspiratory or expiratory (Figure 1) based on their temporal relationship to the ECG-derived respiratory signals (Widjaja *et al.*, 2010) and/or the respiratory variation in pulmonary pressure (Brecher & Hubay, 1955). Pressure and velocity data were ensemble-averaged over the two respiratory periods and WIA was performed as described above. The differences in the ensemble-averaging step, i.e. automated process versus manual beat selection could lead to a slight discrepancy in the wave intensity and

reservoir parameters between free breathing state and the corresponding inspiratory and expiratory values.

Separated waves were quantified by the cumulative area under each wave corresponding to the wave energy per cross sectional area of the artery, over a cardiac period squared. The ratio of backward wave to FCW energy is denoted as the wave reflection index (WRI). The ejection period was taken as the interval between the start of FCW to the end of FDW in systole.

Reservoir-excess pressure analysis

The reservoir pressure was calculated from the raw pressure data using previously described formula (Aguado-Sierra *et al.*, 2008).

(3) $$P_r = P_0 e^{-(ks+kd)t} + P_\infty \frac{b}{a+b}(1-e^{-(ks+kd)t}) + ae^{-(ks+kd)t}\int_0^t P(t')e^{(ks+kd)t'}dt'$$

The reservoir pressure (P_r) is determined by the resistance (R) to outflow from the reservoir, the reservoir compliance (C) and the asymptotic pressure (P_∞). P_∞ is the limit for the exponential decay of reservoir pressure during diastole and corresponds to the pressure at which outflow through the microcirculation would be predicted to be zero; this may exceed the pulmonary venous or left atrial pressure due to the Starling resistor behaviour of the pulmonary circulation (Graham *et al.*, 1982). k_s is the rate constant for reservoir filling (systolic rate constant), which, if it is assumed that waveforms of excess pressure and flow velocity are identical, can be interpreted as the proportionality constant between the arterial inflow and excess pressure. k_b is the rate constant for reservoir emptying (diastolic rate constant), which is assumed to depend on the compliance of the reservoir and the resistance to outflow. The inverse of k_b is τ, the diastolic time constant. P_0 is the pressure at the time t_0 corresponding to the onset of ventricular ejection, i.e. end-diastolic pressure. The excess pressure (P_x) is calculated as the difference between the measured pressure (P) and the reservoir pressure and is related to arterial wave propagation. Reservoir and excess pressures were

quantified by peak P_r (minus diastolic pressure) and P_x and the integral of P_r (minus diastolic pressure) and P_x, respectively. The ratio of excess to reservoir pressure integral is denoted excess-reservoir pressure index (ERPI) (Hametner *et al.*, 2014). In addition, RC_{TPR} was calculated as the product of the total pulmonary resistance (TPR, defined as PAPm divided by cardiac output) and the global arterial compliance (C_p, defined as the ratio of stroke volume to pulmonary pulse pressure) (Lankhaar *et al.*, 2006).

Statistical analysis

Data were analysed for normality using the quantile-quantile plot. Results are expressed as mean (95 % CI) ± SD when normally distributed or median (25 % – 75 % quartile), when non-normally distributed. Statistical comparisons within the same group were performed using a two-way paired Student's t-test for normally distributed data or Wilcoxon signed-rank test for non-parametric data. Differences between the control and PAH group were compared using the unpaired Student's t-test or Welsh's t-test for unequal variances. Wilcoxon rank-sum test. The correlation between P_∞, τ and RC_{TPR} was examined using Spearman's correlation analysis. The level of significance was set at $p < 0.05$[JS1]. All statistical analyses were performed using Stata 13 (StataCorp, Texas, USA).

Results

Respiratory variation

The study was carried out in 10 control subjects (59 [49 – 69] yrs± 14 yrs, 8 males, PAPm: 17 ± 3 [15 – 19] mmHg) and 11 PAH patients (56 [95 % CI: 42 – 70] ± 21 yrs, 2 males, PAPm: 47 [40 – 54] ± 11 mmHg). Inspiratory and expiratory data for each of the groups are summarized in Table 1 and 2, respectively. In both groups, the respiratory variation in heart rate and ejection time did not

differ significantly. PAPm increased by 4.6 (95 % CI: 3.2 – 6.1) ± 0.6 mmHg in controls and 6.0 (95 % CI: 4.9 – 7.1) ± 0.5 mmHg in PAH patients during expiration compared to inspiration. Although not statistically significant, the slightly greater increase in PAPm in PAH patients can be attributed to a small, but significant expiratory increase in the pulmonary arterial pulse pressure (pPAP, by 0.8 ± 0.3 mmHg), which was not observed in controls. Flow velocity appeared to be lower during expiration than inspiration. However, the difference was not statistically significant.

WIA pattern in the pulmonary artery in health and disease has been described previously (Lau *et al.*, 2014). Briefly, a FCW – the incident wave – is observed in early systole corresponding to right ventricular (RV) ejection (Figure 2A). This is followed by a FDW in late systole corresponding to ventricular relaxation prior to the closure of the pulmonary valve. In control subjects, the energy of the mid-systolic backward travelling wave was minimal, while a mid-systolic BCW, i.e. reflection of the preceding FCW, of high energy was observed in PAH patients indicative of downstream vascular impedance mismatch (Table 3). In both groups, the FCW energy was significantly lower during expiration than inspiration (Figure 3) with an expiratory decrease of ~8 6 % for controls and ~65 % for PAH patients, respectively. Wave speed, the energy of the backward travelling wave and WRI remained unchanged throughout the respiratory cycle in both groups (Table 1 and 2).

Valsalva manoeuvre and handgrip exercise

Pressure and velocity measurements and WIA parameters during dynamic stress tests in controls are summarized in Table 3. During Valsalva manoeuvre, PAPm significantly increased by 17 (95 % CI: 9 – 24) ± 10 mmHg while pPAP significantly decreased by 5 (95 % CI: 2 – 7) ± 3 mmHg compared to baseline. Peak velocity was also significantly decreased, while the decrease in mean velocity was not statistically significant. During handgrip exercise, the heart rate and PAPm significantly increased by 12 (95 % CI: 7 – 17)± 7 min^{-1} and 3 (95 % CI: 1 – 5) ± 3 mmHg, respectively, while the increase in mean velocity was not statistically significant.

Examples of ensemble-averaged pressure and velocity waveforms and the corresponding WIA pattern during Valsalva manoeuvre and handgrip exercise are shown in Figure 2B and 2C, respectively. During Valsalva manoeuvre, the ejection period was significantly shorter compared to baseline (Table 3). FCW energy significantly reduced by ~4550 % during Valsalva manoeuvre and ~27 % during handgrip exercise, respectively, while wave speed and wave reflection did not alter significantly. The reduction in wave energy remained statistically significant when non-normalized units were examined. The energy of the backward travelling wave was also significantly reduced in both tests, while WRI and wave speed did not alter significantly.

Reservoir function

Recorded pressure waveforms were not suitable for reservoir-excess pressure analysis in two of the control subjects and one of the PAH patients. Figure 4 illustrates the reservoir-excess pressure model and the separation of the measured pressure into a reservoir and an excess pressure in a representative control subject and PAH patient. The reservoir pressure is the dominant component of the measured pressure in diastole, while the excess pressure is largely responsible for the early systolic pressure rise (Figure 4B and 4C, upper panel). Superimposition of the excess pressure waveform onto the velocity waveform showed the similarity of the two waveforms in the control subject; whereas the excess pressure waveform had a broad top in comparison to the narrow peak of the velocity waveform in the PAH patient (Figure 4B and 4C, lower panel).

In PAH patients, the peak and integral of P_r and P_x were significantly higher compared to controls (Table 4) and the asymptotic pressure, P_∞, was ~25 mmHg greater. The ratio of the excess to reservoir pressure integral (ERPI) was lower in PAH patients (~58 %) than controls (~76 %), but the difference was not statistically significant. The systolic and diastolic rate constants also increased significantly. The time constant,τ, which is the inverse of the diastolic rate constant, was therefore significantly decreased in PAH patients. The product of TPR and C_p, RC_{TPR}, was also

significantly decreased in PAH patients (0.84 [95 % CI: 0.73-0.94] s 0.82 s [0.77 – 1.00 s] versus 1.09 [0.92 – 1.25] s 1.16 s [0.94 – 1.21 s] in controls). Overall, there is a strong and significant correlation between τ and RC_{TPR} (Figure 5), while there was no strong association between P_∞ and RC_{TPR} (controls: rho = -0.36, p = 0.39; PAH: rho = -0.15, p = 0.68) and τ (controls: rho = -0.64, p = 0.09, PAH: rho = -0.36, p = 0.31).

There was little respiratory variation in the reservoir function. In the controls, the diastolic rate constant significantly decreased in expiration compared to inspiration (Table 1), although the difference did not reach statistical signifcance. In PAH patients, the asymptotic pressure and peak P_r were significantly higher during expiration compared to inspiration (Table 2).

During Valsalva manoeuvre, the asymptotic pressure significantly increased by 13 (95 % CI: 1 – 24) $\pm$ 12 mmHg (Table 4) compared to baseline, while peak P_r and P_x significantly decreased ~2 mmHg. P_x integral also significantly decreased, while the decrease in P_r integral and ERPI were not statistically significant. During handgrip exercise, the diastolic rate constant increased significantly, while Tthere were no significant changes in the other reservoir parameters during handgrip exercise (Table 4).

Discussion

By employing WIA and reservoir-excess pressure analysis, the influence of free breathing and dynamic stress tests on pulmonary hemodynamics was explored. We observed that 1) arterial wave energy was lower during expiration compared to inspiration; 2) arterial wave energy decreased during Valsalva Manoeuvre and handgrip exercise; 3) wave speed remained unchanged throughout the respiratory cycle and during dynamic stress tests; 4) the asymptotic, reservoir and excess pressures as well as the systolic and diastolic rate constants were increased in PAH patients compared to controls and; 5) the asymptotic pressure increased and reservoir and excess pressures decreased during Valsalva manoeuvre, while they remained unchanged during handgrip exercise.

Reservoir, excess and asymptotic pressures

Reservoir-excess pressure analysis has been widely applied in the systemic circulation and indices derived from the analysis have been shown to predict cardiovascular events (Davies *et al.*, 2014;Hametner *et al.*, 2014). However, there are only a limited number of studies exploring the reservoir-excess pressure approach in the pulmonary artery in canine models and man (Bouwmeester *et al.*, 2013;Bouwmeester *et al.*, 2014;Ghimire *et al.*, 2016).The reservoir-excess pressure approach was originally developed using both pressure and flow velocity data (Wang et al., 2003). Later, a modified approach using pressure data only was developed (Aguado-Sierra et al., 2008). Both methods produce quantitatively similar results in cases when they have been compared. Flow velocity is rarely measured during clinical as well as experimental settings, while pressure data is widely available. Therefore, in this study, the reservoir-excess pressure analysis was performed using only the measured local pressure data, as this method can be reproduced by most investigators. Nevertheless, a systematic comparison of the two methods for calculating reservoir pressure is warranted, particularly when there are high intensity wave reflections. However, this is beyond the scope of this study.

Reservoir-excess pressure analysis emphasizes the role of the elastic arteries in storing some part of the stroke volume over the cardiac cycle and resolves some apparently anomalous features of wave separation in 1-dimensional models (Parker, 2013). Analogous to its systemic counterpart (Wang *et al.*, 2003), the work done by the right ventricle (RV) can be interpreted as the sum of the work done to fill the reservoir volume and the work done to generate excess pressure (Figure 4A). It should be noted that WIA in this study was applied to the measured pressure rather than the calculated excess pressure as the validity of WIA using the excess pressure remains controversial (Mynard *et al.*, 2012;Segers *et al.*, 2012). As a result of increased RV afterload in PAH, the reservoir and excess pressures increased. The close resemblance of the excess pressure waveform

and the velocity waveform in control subjects is consistent with the low intensity backward travelling wave observed using WIA. In PAH patients, however, while the upslope of the excess pressure waveform corresponded the upslope of the velocity waveform, the two waveforms deviated from one another in mid-systole when the velocity rapidly decreased while peak excess pressure was maintained. This is consistent with the large wave reflection evident in WIA.

It is worth noting that the asymptotic pressure was significantly higher in PAH. P_∞ is the pressure at which the flow out of the large elastic arteries through the microcirculation would be expected to cease. For obvious reasons, P_∞ is difficult to determine in man (Schipke *et al.*, 2003) and remains predominately an empirical parameter that is used as a fitting parameter in the Windkessel model. For simplicity, P_∞ can be set to the venous pressure (Aguado-Sierra *et al.*, 2008;Lankhaar *et al.*, 2008), which results in a significantly poorer fit to the measured diastolic pressure. Arterial pressure at zero flow has been shown to be higher than venous pressure (Magder, 1990), which is generally attributed to a Starling-resistor-like effect of the collapsible microcirculatory vessels (Permutt & Riley, 1963). This "critical closing pressure" is influenced by the interstitial tissue pressure and the active tension generated by vascular smooth muscles (Permutt & Riley, 1963) and it has been suggested that the difference between the arterial P_∞ and venous P_∞ is related to microcirculatory resistance. Hence, the high P_∞ in PAH may be a consequence of increased vascular tone, rarefaction and/or microvascular occlusion (Rabinovitch, 2012).

Systolic and diastolic rate constants

Both the systolic and diastolic rate constants, i.e. the rate of reservoir filling and emptying, were significantly increased in PAH patients. The systolic rate constant is the inverse of the product of the compliance and the ratio between arterial inflow and excess pressure. This ratio is related to, but not necessarily equal to, the characteristic impedance. In PAH, the characteristic impedance has been reported to be increased (Haneda *et al.*, 1983;Laskey *et al.*, 1993) and the total arterial

compliance reduced (Mahapatra *et al.*, 2006). The increased systolic rate constant implies that the decrease in compliance is more prominent than the increase in characteristic impedance.

The diastolic rate constant is the inverse of the diastolic time constant, τ, which represents the exponential reservoir pressure decay during diastole. It describes the relationship between the reservoir compliance and the resistance to outflow from the reservoir, i.e. the large pulmonary arteries. An average τ of ~0.240 s in the PAH patients seems quite short. This may be attributed to the increase in P_∞, which will result in a decrease of the estimated τ (Parragh *et al.*, 2015). RC_{TPR} calculated as the product of TPR and total arterial compliance gives a subtly different, but related estimate of the diastolic pressure decay. It describes the relationship between the arterial compliance and the resistance of the entire pulmonary circulation. Of note, the stroke volume to pulse pressure ratio, a simple and commonly used method to calculate arterial compliance, overestimates the true compliance as it assumes that the proximal pulmonary arteries form a closed system that is exposed to the entire stroke volume without any peripheral outflow (Segers *et al.*, 1999).

The RC-time, calculated as the product of vascular resistance (either TPR or pulmonary vascular resistance, PVR) and compliance, is a much discussed topic in pulmonary hemodynamics. There is evidence that RC-time remains unchanged in individuals with and without pulmonary hypertension and during pulmonary hypertension treatment (Lankhaar *et al.*, 2006;Lankhaar *et al.*, 2008), i.e. there is a fixed inverse relationship between vascular resistance and compliance. This has been interpreted as showing that increased resistance and consequently increased pulmonary pressures lead to decreased arterial compliance by a shift in position on the pressure volume relationship as the tension from the extensible elastin fibres is transferred to the less extensible collagen fibres (London & Pannier, 2010). However, this observation has been contested by several investigators. Studies have shown decreased RC-time with increased pulmonary arterial wedge pressure (Tedford *et al.*, 2012) and in patients with chronic thromboembolic pulmonary hypertension (MacKenzie Ross *et al.*, 2013). Moreover, in a recent study, RC-time has been shown to be increased or

decreased in PAH patients compared to controls depending on whether PVR or TPR is used to derive the value (Hadinnapola *et al.*, 2015). The reported RC-time ranges from 0.21 s (Reuben, 1971) to 0.95 s (Hadinnapola *et al.*, 2015). The large variation is partly explained by the different methods used to derive the value, but also, it challenges the hypothesis of a fixed time constant in the pulmonary circulation. In the present study, both τ and RC_{TPR} were lower in PAH patients, which is inconsistent with the idea of a fixed relationship between compliance and resistance. The decrease in compliance must be more dramatic than the increase in resistance in the PAH patients suggesting that arterial wave reflection and perhaps structural changes in the elastic properties of the pulmonary artery contribute to increased arterial stiffness in addition to the passive change caused by elevated resistance.

Respiratory variations

Respiration has several impacts on the pulmonary circulation; the most evident are changes in pulmonary pressures and flow. The pulmonary circulation is exposed to changes in the intrathoracic pressure during respiration leading to higher pulmonary arterial pressures during expiration than inspiration. The pulmonary flow varies phasically with normal breathing through variations in the venous return. During inspiration, the transmural pressure between the right atrium and the pleura increases and this is accompanied by an increase in venous return and ventricular stroke volume (Brecher & Hubay, 1955) due to the Frank-Starling mechanism. FCW is attributed to RV ejection and consequently, its energy is determined by RV preload, contractility and the properties of the pulmonary artery. Hence, the FCW energy would be expected to be higher during inspiration than expiration in both the control and PAH group as was observed. Moreover, left ventricular contractility appears to be greater during inspiration independent of preload (Karlocai *et al.*, 1998). However, it is not known whether this also occurs in the right ventricle, but if so it could contribute to the larger FCW energy. We did not observe any respiratory variations in pulmonary arterial wave

speed indicating lack of respiratory variation in the local arterial stiffness. Since wave speed is proportional to the characteristic impedance, this is comparable to a previous study that showed no change in pulmonary vascular impedance during spontaneous respiration (Murgo & Westerhof, 1984).

There was little respiratory variation in the reservoir parameters. In the controls, the diastolic rate constant was significantly higher in inspiration compared to expiration. This may be due to a subtle decrease in vascular resistance and/or compliance, both of which may vary in relation to changes in lung volume during spontaneous respiration and artificial ventilation (Brecher & Hubay, 1955;Grant *et al.*, 1991;Castiglioni *et al.*, 1996). The respiratory variation in the diastolic rate constant was abolished in PAH patients, perhaps because normal respiration exerts minimal impact on the high-resistance and low-compliance pulmonary circulation in these patients. In PAH patients, the asymptotic pressure was significantly higher during expiration compared to inspiration which may be ascribed to the increased intrathoracic pressure consistent with the Starling-resistor theory (Permutt & Riley, 1963). The peak reservoir pressure was also increased during expiration, which is presumably due to the increased asymptotic pressure rather than changes in arterial compliance.

Impact of Valsalva manoeuvre and handgrip exercise

We assessed arterial wave behaviour and reservoir function in control subjects during dynamic cardiac stress tests by implementing a modified Valsalva manoeuvre and submaximal isometric handgrip exercise, which affect the ventricular preload and afterload, respectively. Although not routinely used, both manoeuvres have been found to be clinically useful in evaluating cardiovascular diseases (Kivowitz *et al.*, 1971;Felker *et al.*, 2006).

During Valsalva manoeuvre, intrathoracic pressure is increased leading to an increase in the systolic, diastolic and mean pulmonary arterial pressures as well as the diastolic asymptotic pressure. Although not statistically significant, the ~25 % decrease in mean flow velocity implies a

phase II response to Valsalva manoeuvre (Looga, 2005). In this phase, venous return is impeded by compression of the thoracic vena cava and decreased transmural pressure between the right atrium and the pleura leading to decreased RV preload and cardiac output. Accordingly, we observed a substantial decrease in the ejection duration, FCW energy, pPAP, reservoir pressure and excess pressure. The energy of the backward travelling wave reduced accordingly with unchanged WRI.

Isometric handgrip exercise causes sympathetic nerve activation resulting in a minor increase in the heart rate and cardiac output and a pronounced increase in the systemic arterial pressure and vascular resistance (Mitchell & Wildenthal, 1974). The hemodynamic effect of handgrip exercise is immediate. Within 20 seconds, we observed a ~16 % increase in heart rate with a ~5 % statistically insignificant increase of ~5 % in mean flow velocity consistent with a small increase in cardiac output. The pulmonary circulation is also subjected to autonomic nervous regulation. Following direct sympathetic nerve activation in intact animal models, PVR increases (Kadowitz *et al.*, 1974) and arterial compliance decreases (Szidon & Fishman, 1971). Moreover, there is some evidence suggesting that PVR may be increased during isometric exercise (White *et al.*, 2013). However, it is generally believed that exercise related sympathetic activation causes a balanced α-adrenergic vasoconstriction and β-adrenergic vasodilatation in the pulmonary circulation and therefore exerts little net influence on the pulmonary vascular tone (Merkus *et al.*, 2008). Indeed, the ratio of PAPm to mean velocity during handgrip exercise was comparable to baseline values indicative of similar vascular resistance assuming that the cross sectional area of the artery remained the same. The wave speed also remained unchanged suggesting that there was no major change in the local arterial stiffness, which is comparable to a recent study using magnetic resonance imaging to derive pulmonary arterial wave speed during isometric exercise (Weir-McCall *et al.*, 2016). Consistent with the above, the reservoir parameters also remained unchanged. The observed decrease in arterial wave energy can be attributed to the increased heart rate and therefore shorter cardiac cycle duration as wave energy is expressed over a cardiac period squared in this study (equation 2). The

shorter cardiac cycle and therefore shorter diastole also results in less ventricular filling which could contribute to reduced wave energy.

Study limitations

The patient number in the present study is small and therefore, some of the statistical comparisons may be underpowered and statistically significant effects may be exaggerated. For the same reason, we also abstained from performing multivariable analysis and multiple correction testing, although failure to use multiple correction testing may potentially lead to an inflated false positive rate. To recruit completely healthy control subjects in a catheterization laboratory is not feasible. However, we only included individuals without any risk factors for pulmonary vascular disease in the form of lung diseases, left ventricular dysfunction or valvular diseases. In addition, the majority of the control subjects were male, while the majority of PAH patients were female. Although unlikely, we cannot exclude that the uneven distribution in sex may have a small influence on the observed differences in wave propagation and reservoir function between the control and PAH group.

Acquiring high quality velocity measurements was technically demanding, especially in PAH patients, where the pulmonary flow may be highly disturbed resulting in noises and artefacts in the velocity flow signals. Vibration and axial movements of the catheter as well as occasional positioning of the catheter against the arterial wall can also introduce signal artefacts. Thus, careful manipulation of the catheter during the procedure and meticulous data processing were required. We did not use an oesophageal balloon catheter to evaluate the changes in intrapleural pressure during free breathing state and Valsalva manoeuvre, nor did we measure pulmonary arterial wedge pressure and cardiac output during the dynamic stress tests. Therefore, we could not directly determine any variation in the pulmonary distending pressure and PVR under various conditions. We did not measure the systemic blood pressure during handgrip exercise. However, the

hemodynamic effect during handgrip exercise was clear as evidenced by the sudden and significant increase in heart rate. The majority of the PAH patients were on PAH-specific therapy and therefore, we cannot exclude the influence of pharmacological treatment on wave propagation and reservoir function. Furthermore, it would be interesting to investigate the impact of Valsalva manoeuvre and handgrip exercise on arterial wave propagation and reservoir function in PAH patients in future studies.

Inspiratory and expiratory cardiac beats were selected based on the respiratory variation in ECG signal and pulmonary pressure rather than flow velocity. This may explain why the respiratory variation in velocity was statistically insignificant, as variations in the pulmonary flow are most apparent in the subsequent cycle in relation to pressure changes. However, we still observed a higher mean flow velocity in the selected inspiratory cycles in 70 % of the control subjects and 73 % of the PAH patients indicative of respiratory variation in pulmonary flow. Lastly, it was not possible to perform a satisfactory curve fit in order to carry out the reservoir-excess pressure analysis in all the patients because the diastolic pressure waveform could not be described by a decreasing exponential as is assumed in the calculation of the reservoir pressure in all the cases.

Conclusions

This study provides insights into the influence of pulmonary vascular disease, respiration and dynamic stress tests on pulmonary artery wave propagation and reservoir function. Consistent with increased RV afterload in PAH, the reservoir, excess and asymptotic pressures increased, while the diastolic time constant decreased suggestive of intrinsic changes in the pulmonary vasculature. Arterial wave energy decreased during expiration and Valsalva manoeuvre as a result of reduced RV preload caused by changes in the intrathoracic pressure. Submaximal isometric handgrip exercise also caused decreased arterial wave energy in response to shorter cardiac cycles. In

conclusion, variations in the ventricular preload and afterload alter pulmonary arterial wave behaviour and reservoir function.

References

Aguado-Sierra J, Alastruey J, Wang JJ, Hadjiloizou N, Davies J, & Parker KH (2008). Separation of the reservoir and wave pressure and velocity from measurements at an arbitrary location in arteries. *Proc Inst Mech Eng H* **222**, 403-416.

Bouwmeester JC, Belenkie I, Shrive NG, & Tyberg JV (2013). Partitioning pulmonary vascular resistance using the reservoir-wave model. *J Appl Physiol (1985)* **115**, 1838-1845.

Bouwmeester JC, Belenkie I, Shrive NG, & Tyberg JV (2014). Wave reflections in the pulmonary arteries analysed with the reservoir-wave model. *J Physiol* **592**, 3053-3062.

Brecher GA & Hubay CA (1955). Pulmonary blood flow and venous return during spontaneous respiration. *Circ Res* **3**, 210-214.

Castiglioni P, Di RM, Grossoni M, Tommasini R, & Morpurgo M (1996). Does spontaneous respiration alter pulmonary artery input impedance? *Eur Respir J* **9**, 2328-2334.

Davies JE, Lacy P, Tillin T, Collier D, Cruickshank JK, Francis DP, Malaweera A, Mayet J, Stanton A, Williams B, Parker KH, McG Thom SA, & Hughes AD (2014). Excess pressure integral predicts cardiovascular events independent of other risk factors in the conduit artery functional evaluation substudy of Anglo-Scandinavian Cardiac Outcomes Trial. *Hypertension* **64**, 60-68.

Davies JE, Whinnett ZI, Francis DP, Willson K, Foale RA, Malik IS, Hughes AD, Parker KH, & Mayet J (2006). Use of simultaneous pressure and velocity measurements to estimate arterial wave speed at a single site in humans. *Am J Physiol Heart Circ Physiol* **290**, H878-H885.

Felker GM, Cuculich PS, & Gheorghiade M (2006). The Valsalva maneuver: a bedside "biomarker" for heart failure. *Am J Med* **119**, 117-122.

Ghimire A, Andersen MJ, Burrowes LM, Bouwmeester JC, Grant AD, Belenkie I, Fine NM, Borlaug BA, & Tyberg JV (2016). The reservoir-wave approach to characterize pulmonary vascular-right ventricular interactions in humans. *J Appl Physiol (1985)* **121**, 1348-1353.

Graham R, Skoog C, Oppenheimer L, Rabson J, & Goldberg HS (1982). Critical closure in the canine pulmonary vasculature. *Circ Res* **50**, 566-572.

Grant BJ, Fitzpatrick JM, & Lieber BB (1991). Time-varying pulmonary arterial compliance. *J Appl Physiol (1985)* **70**, 575-583.

Hadinnapola C, Li Q, Su L, Pepke-Zaba J, & Toshner M (2015). The resistance-compliance product of the pulmonary circulation varies in health and pulmonary vascular disease. *Physiol Rep* **3**.

Hametner B, Wassertheurer S, Hughes AD, Parker KH, Weber T, & Eber B (2014). Reservoir and excess pressures predict cardiovascular events in high-risk patients. *Int J Cardiol* **171**, 31-36.

Haneda T, Nakajima T, Shirato K, Onodera S, & Takishima T (1983). Effects of oxygen breathing on pulmonary vascular input impedance in patients with pulmonary hypertension. *Chest* **83**, 520-527.

Hollander EH, Dobson GM, Wang JJ, Parker KH, & Tyberg JV (2004). Direct and series transmission of left atrial pressure perturbations to the pulmonary artery: a study using wave-intensity analysis. *Am J Physiol Heart Circ Physiol* **286**, H267-H275.

Kadowitz P, Joiner PD, & Hyman AL (1974). Effect of Sympathetic Nerve Stimulation on Pulmonary Vascular Resistance in the Intact Spontaneously Breathing Dog. *Exp Biol Med (Maywood)* **147**, 68-71.

Karlocai K, Jokkel G, & Kollai M (1998). Changes in left ventricular contractility with the phase of respiration. *J Auton Nerv Syst* **73**, 86-92.

Kivowitz C, Parmley WW, Donoso R, Marcus H, Ganz W, & Swan HJ (1971). Effects of isometric exercise on cardiac performance. The grip test. *Circulation* **44**, 994-1002.

Lankhaar JW, Westerhof N, Faes TJ, Gan CT, Marques KM, Boonstra A, van den Berg FG, Postmus PE, & Vonk-Noordegraaf A (2008). Pulmonary vascular resistance and compliance stay inversely related during treatment of pulmonary hypertension. *Eur Heart J* **29**, 1688-1695.

Lankhaar JW, Westerhof N, Faes TJ, Marques KM, Marcus JT, Postmus PE, & Vonk-Noordegraaf A (2006). Quantification of right ventricular afterload in patients with and without pulmonary hypertension. *Am J Physiol Heart Circ Physiol* **291**, H1731-H1737.

Laskey WK, Ferrari VA, Palevsky HI, & Kussmaul WG (1993). Pulmonary artery hemodynamics in primary pulmonary hypertension. *J Am Coll Cardiol* **21**, 406-412.

Lau EM, Abelson D, Dwyer N, Yu Y, Ng MK, & Celermajer DS (2014). Assessment of ventriculo-arterial interaction in pulmonary arterial hypertension using wave intensity analysis. *Eur Respir J* **43**, 1804-1807.

London GM & Pannier B (2010). Arterial functions: how to interpret the complex physiology. *Nephrol Dial Transplant* **25**, 3815-3823.

Looga R (2005). The Valsalva manoeuvre--cardiovascular effects and performance technique: a critical review. *Respir Physiol Neurobiol* **147**, 39-49.

MacKenzie Ross RV, Toshner MR, Soon E, Naeije R, & Pepke-Zaba J (2013). Decreased time constant of the pulmonary circulation in chronic thromboembolic pulmonary hypertension. *Am J Physiol Heart Circ Physiol* **305**, H259-H264.

Magder S (1990). Starling resistor versus compliance. Which explains the zero-flow pressure of a dynamic arterial pressure-flow relation? *Circ Res* **67**, 209-220.

Mahapatra S, Nishimura RA, Sorajja P, Cha S, & McGoon MD (2006). Relationship of pulmonary arterial capacitance and mortality in idiopathic pulmonary arterial hypertension. *J Am Coll Cardiol* **47**, 799-803.

Merkus D, de Beer VJ, Houweling B, & Duncker DJ (2008). Control of pulmonary vascular tone during exercise in health and pulmonary hypertension. *Pharmacol Ther* **119**, 242-263.

Mitchell JH & Wildenthal K (1974). Static (isometric) exercise and the heart: physiological and clinical considerations. *Annu Rev Med* **25**, 369-381.

Murgo JP & Westerhof N (1984). Input impedance of the pulmonary arterial system in normal man. Effects of respiration and comparison to systemic impedance. *Circ Res* **54**, 666-673.

Mynard JP, Penny DJ, Davidson MR, & Smolich JJ (2012). The reservoir-wave paradigm introduces error into arterial wave analysis: a computer modelling and in-vivo study. *J Hypertens* **30**, 734-743.

Parker KH (2009). An introduction to wave intensity analysis. *Med Biol Eng Comput* **47**, 175-188.

Parker KH (2013). Arterial reservoir pressure, subservient to the McDonald lecture, Artery 13. *Artery Research* **7**, 171-185.

Parragh S, Hametner B, & Wassertheurer S (2015). Influence of an Asymptotic Pressure Level on the Windkessel Models of the Arterial System. *IFAC-PapersOnLine* **48**, 017-022.

Permutt S & Riley RL (1963). Hemodynamics of collapsible vessels with tone: the vascular waterfall. *J Appl Physiol* **18**, 924-932.

Quail MA, Knight DS, Steeden JA, Taelman L, Moledina S, Taylor AM, Segers P, Coghlan GJ, & Muthurangu V (2015). Noninvasive pulmonary artery wave intensity analysis in pulmonary hypertension. *Am J Physiol Heart Circ Physiol* **308**, H1603-H1611.

Rabinovitch M (2012). Molecular pathogenesis of pulmonary arterial hypertension. *J Clin Invest* **122**, 4306-4313.

Reuben SR (1971). Compliance of the human pulmonary arterial system in disease. *Circ Res* **29**, 40-50.

Schipke JD, Heusch G, Sanii AP, Gams E, & Winter J (2003). Static filling pressure in patients during induced ventricular fibrillation. *Am J Physiol Heart Circ Physiol* **285**, H2510-H2515.

Segers P, Brimioulle S, Stergiopulos N, Westerhof N, Naeije R, Maggiorini M, & Verdonck P (1999). Pulmonary arterial compliance in dogs and pigs: the three-element windkessel model revisited. *Am J Physiol* **277**, H725-H731.

Segers P, Swillens A, & Vermeersch S (2012). Reservations on the reservoir. *J Hypertens* **30**, 676-678.

Smolich JJ, Mynard JP, & Penny DJ (2008). Simultaneous pulmonary trunk and pulmonary arterial wave intensity analysis in fetal lambs: evidence for cyclical, midsystolic pulmonary vasoconstriction. *Am J Physiol Regul Integr Comp Physiol* **294**, R1554-R1562.

Su J, Hilberg O, Howard L, Simonsen U, & Hughes AD (2016). A review of wave mechanics in the pulmonary artery with an emphasis on wave intensity analysis. *Acta Physiol (Oxf)* **218**, 239-249.

Szidon JP & Fishman AP (1971). Participation of pulmonary circulation in the defense reaction. *Am J Physiol* **220**, 364-370.

Tedford RJ, Hassoun PM, Mathai SC, Girgis RE, Russell SD, Thiemann DR, Cingolani OH, Mudd JO, Borlaug BA, Redfield MM, Lederer DJ, & Kass DA (2012). Pulmonary capillary wedge pressure augments right ventricular pulsatile loading. *Circulation* **125**, 289-297.

Wang JJ, O'Brien AB, Shrive NG, Parker KH, & Tyberg JV (2003). Time-domain representation of ventricular-arterial coupling as a windkessel and wave system. *Am J Physiol Heart Circ Physiol* **284**, H1358-H1368.

Weir-McCall JR, Kamalasanan A, Cassidy DB, Struthers AD, Lipworth BJ, & Houston JG (2016). Assessment of proximal pulmonary arterial stiffness using magnetic resonance imaging: effects of technique, age and exercise. *BMJ Open Respir Res* **3**, e000149.

White MJ, Lykidis CK, & Balanos GM (2013). The pulmonary vascular response to combined activation of the muscle metaboreflex and mechanoreflex. *Exp Physiol* **98**, 758-767.

Widjaja D, Taelman J, Vandeput S, Braeken MAKA, Otte R, Van den Bergh BRH, & Van Huffel S (2010). ECG-Derived Respiration: Comparison and New Measures for Respiratory Variability. *Computing in Cardiology* **37**, 149-152.

Additional information

Competing interests

None.

Author contributions

The study was carried out at Hammersmith Hospital, Imperial College Healthcare NHS Trust, London. CM, US, ADH and KHP conceived and designed the experiment. CM, JS and LSH collected the experimental data. JS, KHP and ADH performed data analysis and interpretation. JS drafted the paper and all authors revised it critically for important intellectual content. All authors have read and approved the final version of the manuscript.

Funding

This work was supported by St. Mary's Coronary Flow Trust (CFT/13/4001). JS received support from the European Respiratory Society ERS PAH Long-Term Research fellowship (n° LTRF 2013-2183) and Aarhus University Graduate School. ADH received support from a National Institute for Health Research Biomedical Research Centre Award to University College London Hospital and a British Heart Foundation grant (BHF PG/13/6/29934). LSH received support from a National Institute for Health Research Biomedical Research Centre Award to Imperial College Healthcare NHS Trust.

Table 1: Inspiratory and expiratory data for control subjects

	Inspiration	Expiration	p
Measurements			
Heart rate (min^{-1})	79 (69-88)	77 (67-86)	0.19
Ejection time (ms)	360 (332-388)	345 (308-347)	0.09
Systolic PAP (mmHg)	23 (21-24)	27 (25-30)	<0.01*
Diastolic PAP (mmHg)	9 (8-10)	14 (12-16)	<0.01*
Mean PAP (mmHg)	14 (13-15)	18 (16 -20)	<0.01*
Mean velocity ($cm \cdot s^{-1}$)	38.4 (28.5-48.4)	35.7 (27.7-43.8)	0.10
Max velocity ($cm \cdot s^{-1}$)	65.8 (50.6-81.1)	62.7 (47.9-77.6)	0.10
Wave intensity analysis			
Wave speed ($m \cdot s^{-1}$)	2.40 (1.75-3.05)	2.36 (1.88-2.84)	0.80
FCW (10^3 $J \cdot m^{-2}$)	4.27 (2.89-5.63)	3.92 (2.56-5.29)	0.01*
FDW (10^3 $J \cdot m^{-2}$)	1.62 (0.96-2.28)	1.55 (0.79-2.31)	0.46
BW (10^3 $J \cdot m^{-2}$)	0.22 (0.10-3.37)	0.23 (0.10-0.36)	0.65
WRI (%)	5.18 (3.05-7.31)	6.56 (3.24- 9.88)	0.14
Reservoir-excess pressure analysis			
Peak P_r (mmHg)	6.81 (5.33-8.29)	6.41 (5.36-7.45)	0.46
P_r integral (mmHg·s)	2.34 (1.76-2.92)	2.22 (1.69-2.75)	0.49
Peak P_x (mmHg)	7.52 (5.87-9.17)	8.32 (7.30-9.35)	0.14
P_x integral (mmHg·s)	1.29 (0.85-1.73)	1.44 (1.19-1.70)	0.22
k_s (s^{-1})	10.6 (4.3-16.9)	6.86 (4.86-8.86)	0.16
k_d (s^{-1})	3.14 (1.45-4.83)	1.70 (0.91-2.49)	0.07
τ (s)	0.47 (0.16-0.78)	0.76 (0.42-0.11)	0.14
P_∞ (mmHg)	7.38 (4.51-10.26)	9.03 (4.21-13.85)	0.55
ERPI (%)	58.8 (37.2-80.4)	69.7 (49.3-90.1)	0.24

Results are presented as mean (95 % CI) ± SD or median (25 % – 75 % quartile). Abbreviations:

BW: backward wave (appears as a backward decompression wave in three of the subjects and backward compression wave in the rest), ERPI: excess reservoir pressure index, FCW: forward compression wave, FDW: forward decompression wave, k_d: diastolic rate constant, k_s: systolic rate constan, PAP: pulmonary arterial pressure, P_r: reservoir pressure (minus diastolic pressure), P_x: excess pressure, P_∞: asymptotic pressure, τ: diastolic time constant, U: flow velocity, WRI: wave reflection index. *$p < 0.05$ versus inspiration.

Table 2: Inspiratory and expiratory data for pulmonary arterial hypertension patients

	Inspiration	Expiration	p
Measurements			
Heart rate (min^{-1})	81 (76- 86)	81 (76-86)	0.26
Ejection time (ms)	328 (308-347)	332 (314-351)	0.36
Systolic PAP (mmHg)	73 (62-84)	78 (67-90)	<0.01*
Diastolic PAP (mmHg)	29 (22-36)	35 (29-42)	<0.01*
Mean PAP (mmHg)	44 (36-51)	50 (42-57)	<0.01*
Mean velocity ($cm \cdot s^{-1}$)	21.9 (15.7-28.0)	21.5 (14.9-28.0)	0.26
Max velocity ($cm \cdot s^{-1}$)	42.7 (29.7-55.7)	40.9 (28.6-53.2)	0.12
Wave intensity analysis			
Wave speed ($m \cdot s^{-1}$)	12.0 (8.1-16.0)	11.6 (7.9-15.2)	0.42
FCW (10^3 $J \cdot m^{-2}$)	7.10 (5.34-8.85)	6.65 (4.92-8.39)	0.04*
FDW (10^3 $J \cdot m^{-2}$)	2.50 (1.63- 3.37)	2.46 (1.65-3.28)	0.82
BCW (10^3 $J \cdot m^{-2}$)	1.77 (1.07- 2.48)	1.71 (1.33-2.09)	0.85
WRI (%)	25.5 (18.0-33.0)	28.0 (21.1-34.9)	0.56
Reservoir-excess pressure analysis			
Peak P_r (mmHg)	26.1 (21.3-30.8)	28.3 (23.3-33.2)	0.03*
P_r integral (mmHg·s)	7.92 (6.15-9.69)	8.66 (7.01-10.32)	0.09
Peak P_x (mmHg)	23.0 (18.8-27.3)	22.7 (18.4-26.9)	0.59
P_x integral (mmHg·s)	4.47 (3.47-5.47)	4.37 (3.46-5.29)	0.54
k_s (s^{-1})	10.9 (8.9-12.8)	11.5 (9.6-13.3)	0.35
k_d (s^{-1})	5.09 (3.38-6.80)	4.79 (3.53-6.05)	0.29
τ (s)	0.24 (0.15-0.32)	0.24 (0.16-0.32)	0.36
P_∞ (mmHg)	28.8 (22.1-35.5)	33.0 (26.4-39.5)	<0.01*
ERPI (%)	59.4 (44.7-74.2)	51.7 (41.9-61.4)	0.08

Results are presented as mean (95 % CI) ± SD or median (25 % – 75 % quartile). Abbreviations: BCW: backward compression wave, ERPI: excess reservoir pressure index, FCW: forward compression wave, FDW: forward decompression wave, k_d: diastolic rate constant, k_s: systolic rate constant, PAP: pulmonary arterial pressure, P_r: reservoir pressure (minus diastolic pressure), P_x:

excess pressure, P_∞: asymptotic pressure, τ: diastolic time constant, U: flow velocity, WRI: wave reflection index. * $p < 0.05$ versus inspiration.

Table 3: Pressure and velocity measurements and wave intensity parameters during dynamic stress tests

	PAH	Control Baseline	p	Control Valsalva	p	Control Handgrip	p
Measurements							
Heart rate (min^{-1})	81 (76-86)	73 (68-78)	0.03*	78 (63-93)	0.30	85 (77-93)	<0.01†
Ejection time (ms)	331 (311-352)	352 (321-383)	0.21	312 (283-341)	0.03†	346 (329-363)	0.56
sPAP (mmHg)	76 (65-87)	26 (23-28)	<0.01*	39 (32-47)	0.01†	27 (24-31)	0.11
dPAP (mmHg)	33 (27-40)	12 (10-14)	<0.01*	31 (23-39)	<0.01†	15 (12-18)	0.01†
PAPm (mmHg)	47 (40-54)	17 (15-19)	<0.01*	34 (26-42)	<0.01†	20 (17-23)	0.01†
U_{mean} ($cm \cdot s^{-1}$)	21.0 (14.6-27.3)	33.8 (24.5-43.2)	0.02*	24.8 (16.5-33.0)	0.09	35.6 (28.6-42.5)	0.30
U_{max} ($cm \cdot s^{-1}$)	40.9 (28.6-53.1)	63.0 (47.9-78.1)	0.01*	45.3 (32.9-57.7)	0.02†	62.8 (48.8-76.8)	0.91
Wave intensity analysis							
Wave speed ($m \cdot s^{-1}$)	12.4 (8.4-16.3)	2.52 (1.96-3.09)	<0.01*	2.22 (1.67- 2.77)	0.09	2.68 (2.12-3.23)	0.20
FCW (10^3 $J \cdot m^{-2}$)	6.75 (4.96-8.54)	3.92 (2.55-5.29)	0.01*	2.17 (1.11-2.23)	0.03†	2.85 (2.09-3.61)	0.01†
FDW (10^3 $J \cdot m^{-2}$)	2.42 (1.64-3.21)	1.48 (0.85-2.10)	0.05	1.03 (0.32-1.75)	0.06	1.15 (0.83-1.48)	0.06
BW (10^3 $J \cdot m^{-2}$)	1.72 (1.31-2.13)	0.23 (0.10-0.35)	<0.01*	0.11 (-0.02-0.25)	0.02†	0.10 (0.04-0.16)	0.05
WRI (%)	27.4 (20.7-34.0)	7.01 (3.40-10.62)	<0.01*	4.72 (0.60-8.84)	0.32	4.88 (0.93-8.82)	0.14

Results are presented as mean (95 % CI) ± SD or median (25 % – 75 % quartile). Abbreviations: PAP: pulmonary arterial pressure, FCW: forward compression wave, FDW: forward decompression wave, BW: backward wave. *$p < 0.05$ versus PAH. †$p < 0.05$ versus baseline.

Table 4: Reservoir parameters for PAH patients and control subjects at rest and during dynamic stress tests

	PAH	Control Baseline	p	Control Valsalva	p	Control Handgrip	p
Peak P_r (mmHg)	27.0 (22.1-31.9)	6.35 (5.35-7.34)	<0.01*	4.42 (3.64-5.20)	0.03†	6.91 (4.70-9.12)	0.3
P_r integral (mmHg·s)	7.89 (6.04-9.75)	2.19 (1.67-2.70)	<0.01*	1.71 (1.16-2.26)	0.23	2.37 (1.54-3.20)	0.4
Peak P_x (mmHg)	24.2 (17.5-31.0)	8.44 (7.44-9.45)	<0.01*	6.01 (4.27-7.74)	<0.01†	7.58 (6.34-8.81)	0.2
P_x integral (mmHg·s)	4.27 (3.37-5.26)	1.53 (1.27-1.79)	<0.01*	0.95 (0.54-1.36)	<0.01†	1.31 (0.96-1.66)	0.2
k_s (s^{-1})	11.5 (9.7-13.4)	6.55 (4.92-8.17)	<0.01*	7.13 (3.99-10.28)	0.35	9.35 (4.59-14.12)	0.2
k_d (s^{-1})	5.01 (3.68-6.33)	1.58 (1.12-2.04)	<0.01*	1.41 (-0.05-2.88)	0.87	2.17 (1.29-3.06)	0.05
τ (s)	0.24 (0.15-0.32)	0.70 (0.50-0.90)	<0.01*	1.43 (0.52-2.33)	0.11	0.64 (0.24-1.05)	0.0
P_∞ (mmHg)	33.2 (26.2-40.2)	8.53 (4.67-12.40)	<0.01*	20.9 (5.9-35.8)	0.03†	11.5 (7.5-15.5)	0.0
ERPI (%)	58.1 (42.3-73.9)	76.3 (50.4-102.2)	0.17	56.7 (36.9-76.5)	0.17	63.0 (40.5-85.5)	0.28

Results are presented as mean (95 % CI) ± SD or median (25 % – 75 % quartile). Abbreviations: ERPI: excess reservoir pressure index, k_d: diastolic rate constant, k_s: systolic rate constant, PAH: pulmonary arterial hypertension, P_r: reservoir pressure (minus diastolic pressure), P_x: excess pressure, P_∞: asymptotic pressure, τ: diastolic time constant. *$p < 0.05$ versus PAH. †$p < 0.05$ versus baseline.

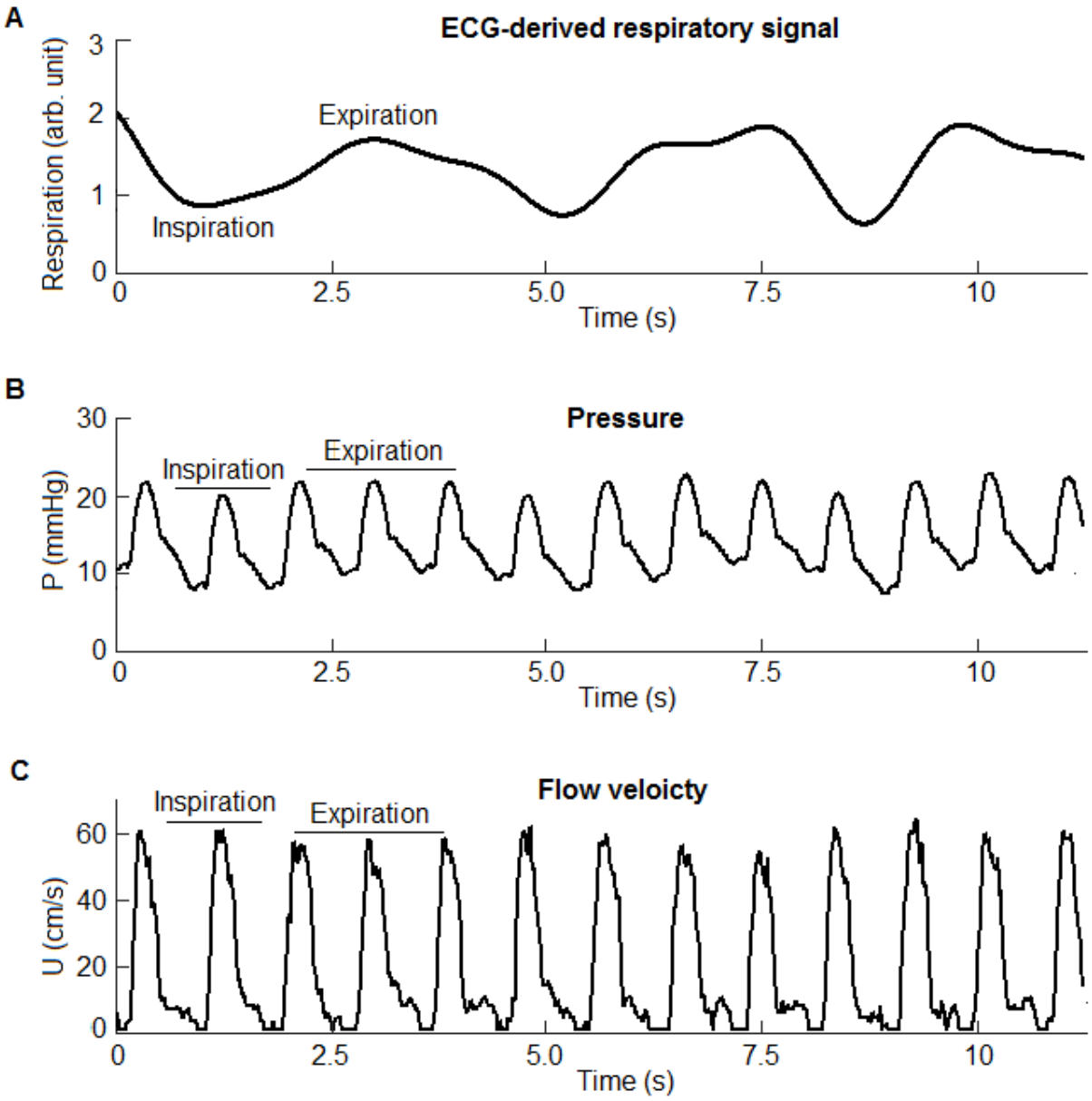

Figure legends

Figure 1. Pressure and velocity recording from a representative control subject

ECG-derived respiratory signal (A) is based on the respiratory variation in the R–S amplitude and corresponds temporally to the respiratory variation in pulmonary pressure (B) and flow velocity (C).

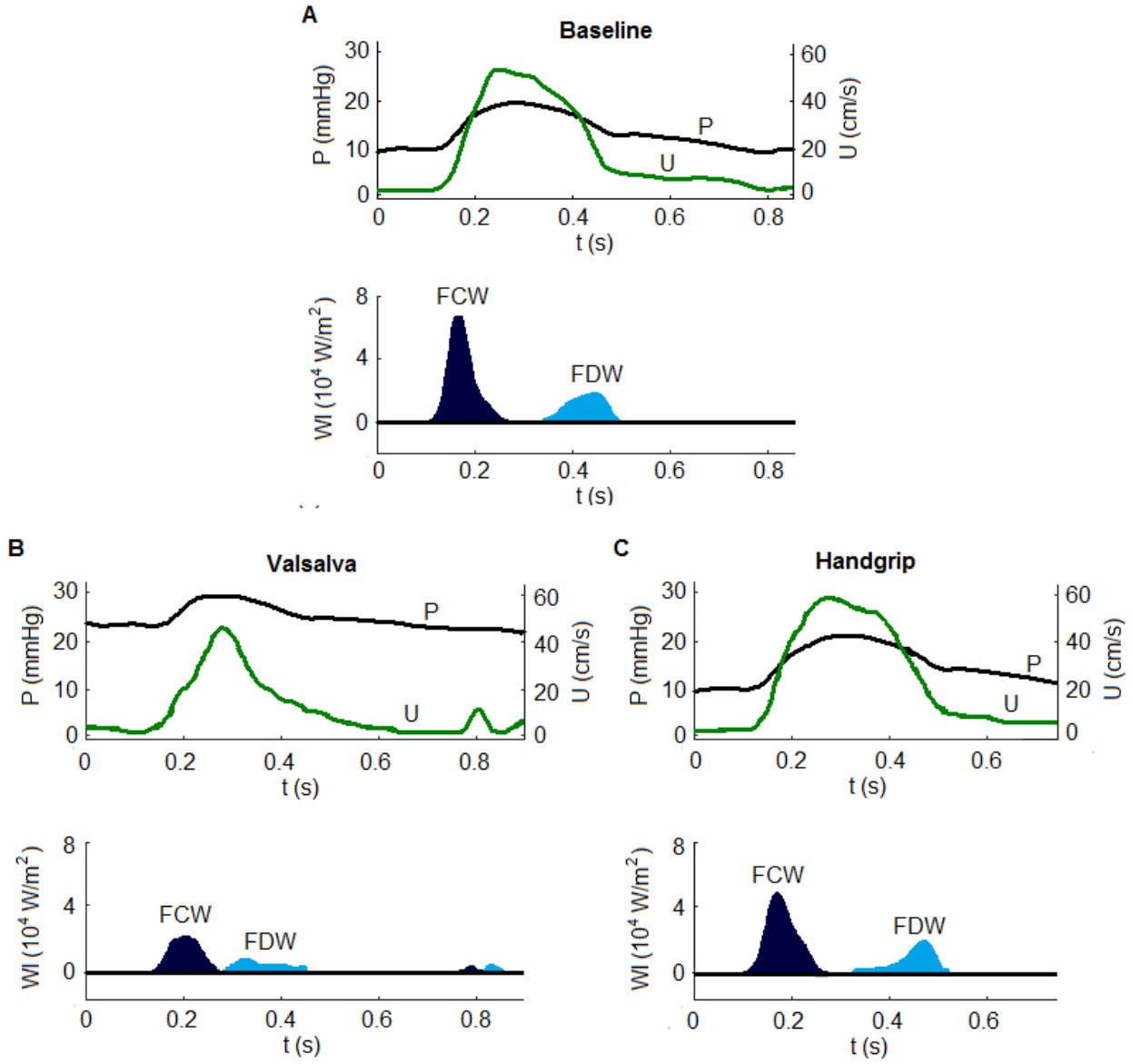

Figure 2. Wave intensity pattern

Ensemble-averaged pressure (P, black line) and flow velocity (U, green line) and wave intensity for a representative control subject at baseline (A), during Valsalva manoeuvre (B) and during handgrip exercise (C) are shown. There is a forward compression wave (FCW, dark blue) associated with right ventricular ejection and a forward decompression wave (FDW, light blue) related to ventricular relaxation, while there was minimal backward travelling wave present. The magnitude of FCW decreased during dynamic stress tests, the time interval between FCW and FDW was reduced during Valsalva manoeuvre as a result of shorter ejection period and the cardiac duration decreased during handgrip exercise.

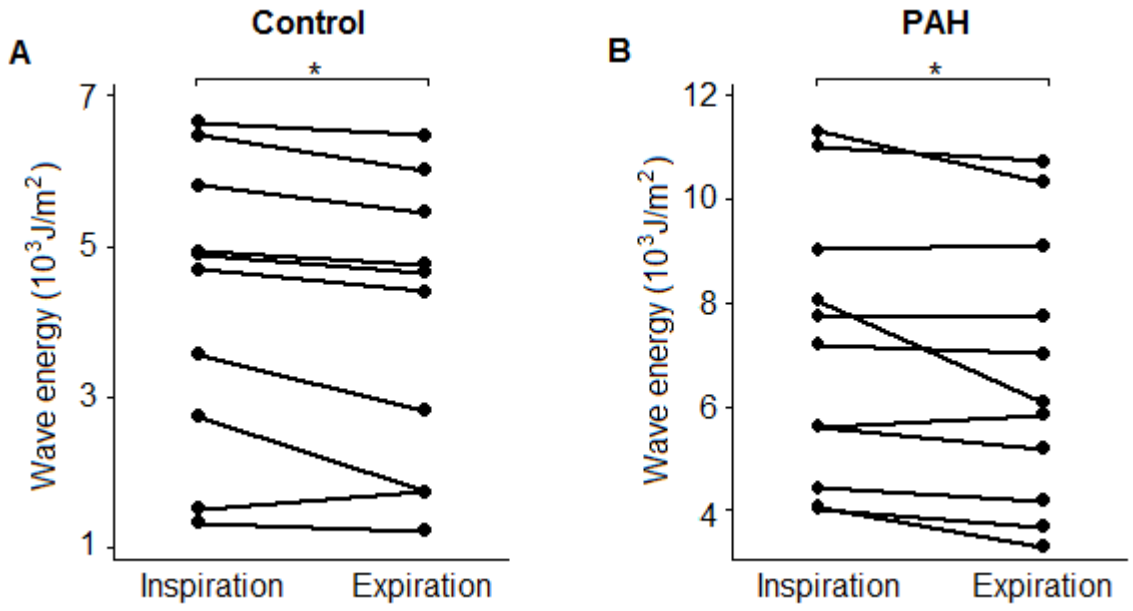

Figure 3. Arterial wave energy

Wave energy of the forward compression wave was greater in inspiration compared to expiration in both controls (A) and patients with pulmonary arterial hypertension (PAH, B). *$p < 0.05$.

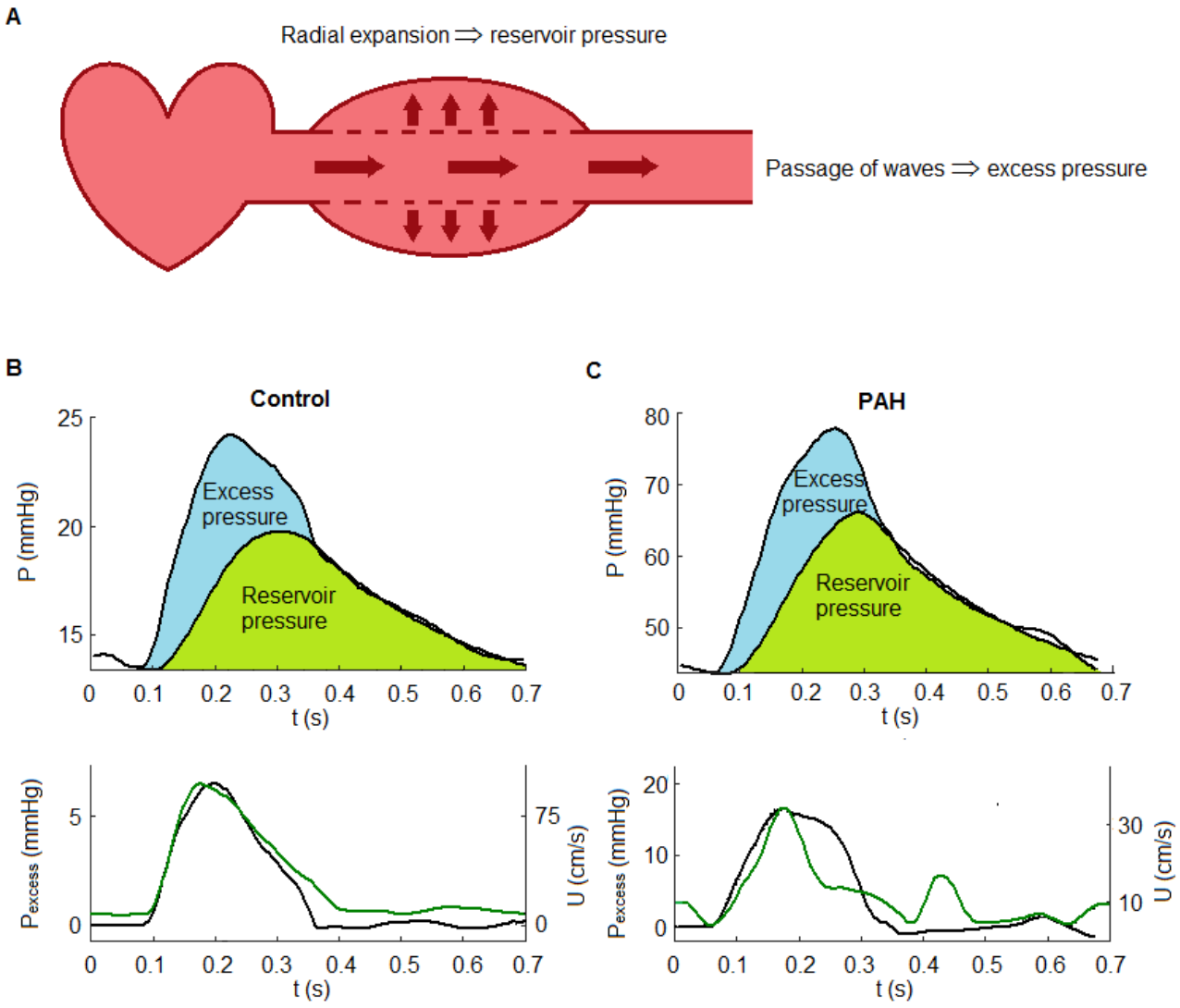

Figure 4. Reservoir-excess pressure analysis

The reservoir-excess pressure model is illustrated in A. The measured pressure was separated into a reservoir pressure and an excess pressure in a representative control subject (B, upper panel) and a patient with pulmonary arterial hypertension (PAH, C, upper panel). Both the reservoir and excess pressures increased in PAH (note the scale difference). In the lower panel of B and C, the excess pressure (black line) was compared to the flow velocity profile (green line, scaled so that the peak of the waveforms coincide).

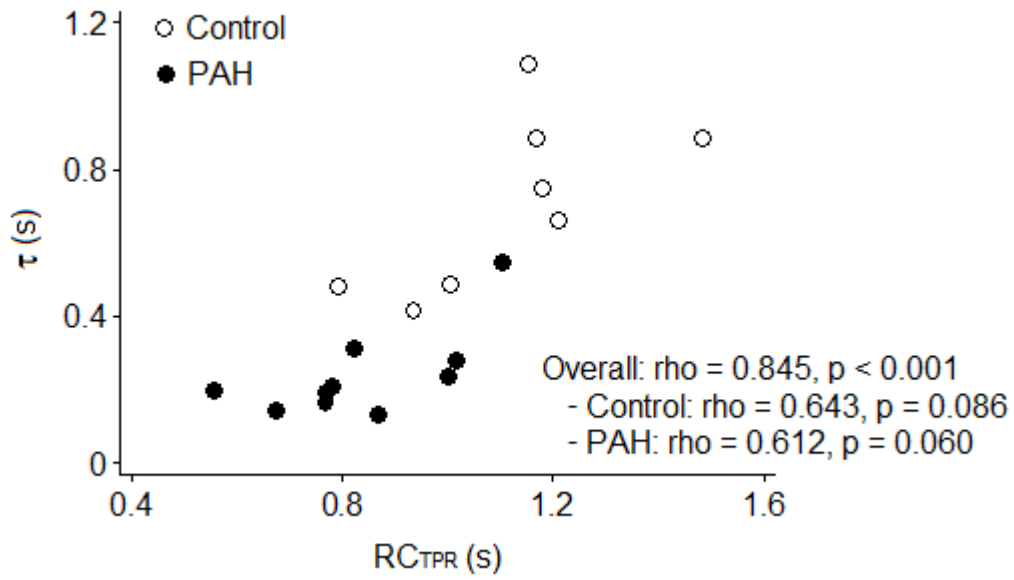

Figure 5: Relationship between diastolic time constants τ and RC_{TPR}

τ is the inverse of the diastolic rate constant and RC_{TPR} is product of total pulmonary vascular resistance and compliance. PAH: pulmonary arterial hypertension.